Fine-scale habitat preference of green sturgeon (Acipenser medirostris) within three spawning locations in the...

Article *in* Canadian Journal of Fisheries and Aquatic Sciences · July 2017

DOI: 10.1139/cjfas-2017-0072

12 authors, including:

Richard Reid Mcdonald
United States Geological Survey

Paul J. Kinzel
United States Geological Survey

E. A. Mora
NOAA National Marine Fisheries Service

Jonathan Mark Nelson
United States Geological Survey

Fine-scale habitat selection of green sturgeon (*Acipenser medirostris*) within three spawning locations in the Sacramento River, California

Wyman[1], M.T., Thomas[1], M.J., McDonald[2], R.R., Hearn[1,3], A.R., Battleson[1], R.D., Chapman, E.D[1]., Kinzel[2], P., Minear[4], J.T., Mora[1,] , E.A., Nelson[2], J.M., Pagel[1], M.D., and Klimley[1], A.P.

[1]Department of Wildlife, Fish, and Conservation Biology. University of California, Davis, CA, USA

[2]U.S. Geological Survey, Geomorphology and Sediment Transport Laboratory, Golden, CO, USA

[3]Universidad San Francisco de Quito, Ecuador

[4]Cooperative Institute for Research in Environmental Sciences (CIRES), University of Colorado

Key words: habitat suitability, green sturgeon, *Acipenser medirostris*, hydraulic modeling, acoustic fish positioning

ABSTRACT

Vast sections of the Sacramento River have been listed as critical habitat by the National Marine Fisheries Service for green sturgeon spawning (*Acipenser medirostris*), yet spawning is known to occur at only a few specific locations. This study reveals the range of physical habitat variables selected by adult green sturgeon during their spawning period. We integrated fine-scale fish positions, physical habitat characteristics, discharge, bathymetry, and simulated velocity and depth using a 2-dimensional hydraulic model (FaSTMECH). The objective was to create habitat suitability curves for depth, velocity, and substrate type within three known spawning locations over two years. An overall cumulative habitat suitability score was calculated that averaged the depth, velocity, and substrate scores over all fish, sites, and years. A weighted usable area (WUA) index was calculated throughout the sampling periods for each of the three sites. Cumulative results indicate that the microhabitat characteristics most preferred by green sturgeon in these three spawning locations were velocities between 1.0-1.1 m/s, depths of 8-9 m, and gravel and sand substrate. This study provides guidance for those who may in the future want to increase spawning habitat for green sturgeon within the Sacramento River.

INTRODUCTION

Sturgeon species that inhabit lakes, estuaries, and ocean make upstream migrations in rivers to spawn within the headwaters of rivers. The geomorphology and physical properties of the spawning sites have been well described for the gulf sturgeon *Acipenser oxyrhynchus* (Fox et al. 2000), lake sturgeon, *Acipenser fulvescens* (LeHaye et al. 1992, Knight et al. 2002, Dougherty et al. 2007), pallid sturgeon, *Scaphirhynchus albus* (DeLonay et al. 2016), and white sturgeon, *Acipenser transmontanus* (Parsley et al. 1993). While coarse-scale descriptions of spawning habitat have been described for the green sturgeon (Poytress et al. 2015, USFW 2013), no studies have yet described fine-scale habitat selection within these sites. This species is among the most adversely affected species in North America due to inadequate management, restoration capacity, and poorly defined habitat criteria (Pikitch et al. 2005).

There are two genetically distinct populations of green sturgeon found along the coast, bays, and rivers of western North America: the northern and southern Distinct Population Segments (nDPS and sDPS, respectively) [Israel et al. 2004]. The latter population has been in serious decline primarily due to watershed degradation, water diversions, and dams (Adams et al. 2007; Heublein et al. 2009; Mora et al. 2009), resulting in the listing of sDPS green sturgeon as federally threatened (NMFS, 2006). The sDPS population and its recruitment largely relies on spawning habitats found in the main stem of the Sacramento River (Brown 2007; Heublein et al. 2009; Thomas et al. 2014; Poytress et al. 2015), although spawning has recently been documented in one of its major tributaries (Seesholtz et al. 2015). Successful management of green sturgeon is highly dependent upon more expansive research (NMFS 2015), particularly on its reproductive ecology given the biologically recent large-scale trend in spawning habitat loss (Adams et al. 2007; Mora et al. 2009).

Currently, vast sections of the Sacramento River have been listed as critical habitat for green sturgeon spawning (NMFS 2009, 2015), yet spawning is known to occur at these and only a few other locations based on egg and larval sampling (United States Fish and Wildlife Service [USFWS] 2013; Poytress et al. 2015). What range of physical habitat variables exists at these confirmed spawning sites? How do green sturgeon utilize the available microhabitat during their spawning period? Do they prefer a particular depth, substrate type, and/or flow regime? The objective of this study was to address these important questions by modeling habitat selection based on three common descriptors of microhabitat (depth, velocity, and substrate) in combination with fine-scale fish movement data within known spawning aggregation sites in the Sacramento River.

METHODOLOGY

Study sites

Within the main stem of the Sacramento River in Northern California, the current putative spawning grounds of sDPS green sturgeon occur from approximately Redding near the Keswick Dam down to near Hamilton City. In general, this diverse riverine habitat exhibits meandering alluvial habitat to constrained bedrock morphology and a mix of agricultural, residential, and natural land uses along the banks. We described green sturgeon habitat selection at three locations as follows: Site A – rkm 377, Site B – rkm 407.5, and Site C – rkm 426. These sites were shown to be spawning sites based on net tows and egg mats in other studies (Poytress et al. 2015) (Fig 1). All study sites are in close proximity to a tributary stream and are characterized by dynamic flows, variable bathymetry extending greater than 5 m deep, and a mixture of substrate types with gravel and cobble predominant amongst scoured areas of boulder and bedrock and areas of sandy deposits. Overall, Sites A and C are relatively similar in substrate and channel bank morphology, whereas Site B has a narrower channel and more complex bedrock formations along the banks. These specific locations were chosen based on previous active telemetry that indicated extended residence of adult green sturgeon at these sites during the spawning season (Thomas et al. 2014). Spawning was confirmed at these sites using egg mat surveys (Poytress et al. 2015).

Acoustic telemetry

Adult green sturgeon were captured and tagged between 2008 and 2012 in four watersheds. They consisted of the Sacramento River, CA, Umpqua River, OR, Chehalis River, WA, and Columbia River, WA/OR (see Matt Pagel, Biotelemetry Laboratory, UC Davis, for metadata and sources of tags). During the tagging procedure, a coded ultrasonic transmitter (VEMCO V16-6X) was surgically inserted into the abdominal cavity of each fish (see Thomas et al. 2014 for details on tagging procedure). All surgical procedures performed during tag implantation within the green sturgeon were reviewed and authorized by the University of California, Davis, Animal Care and Use Committee (IACUC) in Protocol 16154. Fish positions were calculated with fine-scale resolution at the three sites on the Sacramento River during the 2011 and 2012 spawning seasons using the VEMCO Positioning System (VPS; VEMCO Division of AMIRIX Systems, Halifax, Nova Scotia, Canada), an array of underwater acoustic receivers. The receivers making up the VPS were deployed along each bank of the river so that they were able to record positions of sturgeon as they moved throughout these aggregation sites (Poytress et al. 2013; Thomas et al. 2014). At each site, the VPS was composed of four to five hydrophone receivers (VEMCO, VR2Ws with co-located 69 kHz transmitters (“sync tags”) attached to each receiver and a separate 69 kHz transmitter (“reference tag”) [VEMCO, V13 and V16] moored in the middle of the receiver locations. These had intervals ranging from 600 to 800 seconds not to interfere with the coded pulse trains from the transmitters on the sturgeon (Fig. 2). The transmitters on the sturgeon (VEMCO V16) emitted uniquely coded ultrasonic signals at random intervals of mainly 60 to 90 seconds while the receivers recorded the identity of the unique transmitter and the date and time of its detection. The locations of all receivers and transmitters were recorded using a Trimble GeoExplorer XT (Trimble Navigation Limited, Sunnyvale, CA) with sub meter positioning accuracy.

Tag detections from each receiver were downloaded and subsequently post-processed by VEMCO to derive fish positions with an associated horizontal positioning error (HPE) estimate calculated for each position. HPE is a unitless estimate of error: lower HPE values correspond to smaller scatter of calculated positions (i.e., higher precision) (Smith 2013). Fish positions with HPE > 8 m were removed from the dataset in order to increase the accuracy of the fish positions used in subsequent analyses (see Scheel and Bisson 2012; Coates et al. 2013). In general, VPS performance decreased at discharge levels greater than approximately 350 to 400 m^3/s, as observed through fewer detections, smaller proportions of detections contributing to positions, and reduced positioning efficiency. The mean discharge of water at the United States Geological Survey (USGS) streamgage nearest to the three study sites (gage number 11377100, above Bend Bridge near Red Bluff) was 390.8 m^3/sec during the winter of 2011 and 266.1 m^3/sec during the winter of 2012 (U.S. Geological Survey, 2014).

Habitat measures

Discharge, bathymetry, and water-surface elevation data were recorded at all three sites on 22-24 May 2013 using an Acoustic Doppler Current Profiler (ADCP) [River Surveyor M9, SonTek, San Diego, CA] to develop and calibrate the hydraulic model. The ADCP was mounted to an aluminum boat at a fixed transducer depth of 0.2 – 0.5 m. Position was measured using a co-located global positioning system (GPS) [Trimble R7, Real Time Kinematic] with centimeter positioning accuracy. At each site, we measured discharge using the ADCP, by completing three to four cross-sections near the top of the reach. Following the discharge measurement, we recorded a longitudinal water-surface elevation. The paired discharge and water-surface elevation profiles were used to calibrate the hydraulic model at each site. The channel bathymetry was measured by completing a perimeter sweep near the water's edge and multiple cross-sections through the reach in a zig-zag pattern. This pattern resulted in measured cross-sections that were separated by less than one channel width apart.

A stage-discharge relationship is required at each site in order to model flow correctly. The discharges were obtained from the nearest gage to each of the three sites (USGS gage number 11377100). This gage is approximately 36 km and 9 km upstream from Site A and B respectively, and 7 km downstream from Site C. In addition, pressure sensors (HOBO, Onset Computer Corporation) were deployed at four locations within each site, three in the channel and one on the closest shore from 8 March to 11 June 2014. The on-land pressure transducers were used to provide an atmospheric pressure correction for the in-channel transducers. The location and datum of each pressure sensor was determined with the GPS. The resulting water-surface elevation at the transducers located at the downstream end of each site was compared to the USGS gage stage data (U.S. Geological Survey 2014). Travel times of approximately -0.5, 1.75, and 3.5 hours for sites A, B, and C, respectively, were determined based on the time separating peak in measured stage, recorded in the pressure sensors at each site, with the corresponding peak in measured discharge at the USGS gage of 741.9 m^3/s on 10 March 2014. The shifted discharge was plotted against the measured stage at each location and a third-order polynomial was fit to the data. This functional relationship was used to define the stage-discharge boundary condition at each location. Because of the relatively short travel time between the USGS gage and the three sites, we modeled discharge using the gage's recorded daily discharge values. The simulated discharge at each reach was interpolated within 12-hour time steps.

At each site, we used a Dual Frequency Identification Sonar (DIDSON) [Sound Metrics Corporation, Lake Forest Park, WA] to visualize and classify substrate types for inclusion in the selection models. The DIDSON recorded continuous high-quality acoustic images of the channel bottom along with concurrent GPS positions logged by a Trimble GPS on 27-28 June 2013. We made six longitudinal transects at Site A, three at Site B, and five at Site C based on the width of the channel and the complexity of the substrate. The acoustic images of the substrate collected by DIDSON were inspected using Sound Metrics software. Substrate types were categorized into the following size classes based on a modified Wentworth particle size scheme (Wentworth 1922): sand (0.06–2 mm dia.), gravel (3–64 mm dia.), cobble (65–256 mm dia.), and boulder (0.257–3 m dia.), with any boulders larger than 3 m classified as bedrock. Additionally, we characterized large submerged objects (e.g., trees) as snags, although these were only present in Site A. The positions of the substrate points were loaded into ArcGIS 10.1 (ESRI 2012) for conversion into polygon shapefiles. Points of uncertainty were re-examined *in situ* using an underwater video camera. We also conducted random spot tests to quantify the accuracy of our substrate classification procedure, resulting in the correct match of 80.9% of test points.

Habitat flow model

We used the Flow and Sediment Transport with Morphologic Evolution of Channel Hydrology (FaSTMECH) model (Nelson and McDonald, 1996; Nelson et al. 2016a) within the International River Interface Cooperative modeling interface (Nelson et al. 2016b) for this study. The model is 2-D and flow is assumed to be incompressible, hydrostatic, and quasi-steady. Thus, the simulation of the time-varying discharge hydrograph during the telemetric sampling period is approximated as a piecewise sequence of steady flows. FaSTMECH is quasi-three-dimensional, which means the model solves the vertically averaged equations expressing conservation of mass and momentum, and then uses that solution along with similarity vertical structure functions and the streamlines of the vertically averaged flow solution to assign vertical structure along those streamlines. In addition, the model computes secondary flow components associated with channel or streamline curvature perpendicular to those streamlines. The model equations are solved on a curvilinear orthogonal coordinate system (the so-called “channel-fitted” coordinate system). This model has been used and verified extensively on a wide variety of rivers (Lisle et al. 2000; Conaway and Moran 2004; Logan et al. 2011; Harrison et al. 2011; Legleiter et al. 2011; Hafs et al. 2014).

The minimum requirements for the development and calibration of the FaSTMECH model are topography and boundary conditions, typically water-surface elevation at the downstream boundary and discharge at the upstream boundary. The model was developed on an approximately 2 X 2 meter curvilinear orthogonal grid using the measured bathymetric data, supplemented with available LiDAR data collected in February and March 2010 (CVFED, 2014) to provide bank topography. The model was calibrated using the measured longitudinal profiles of water-surface elevation and the associated measured discharge (357, 413, and 401 m^3/s for Site A, Site B, and Site C respectively) collected at each of the three sites on 22-24 May 2013.

Following the calibration of the hydraulic model for each site, the flow was simulated during the spawning season in 2011 and 2012. At each site, the flow was simulated between 15 May – 15 July in 2011 and 16 April – 27 June in 2012. These date ranges span the telemetered fish positions at each site. We simulated flow on a 12-hour time step using the stage-discharge relationship developed at each site described previously. The resulting simulations provide time specific velocity and depth at each node of the computational grid. To facilitate the calculation of the microhabitat metrics, substrate types were also interpolated to the computational grid nodes, although the channel morphology and substrate were assumed to be constant throughout the simulation.

Habitat suitability values

In this section we describe the procedure to calculate the available and selected physical habitat metrics as determined from the simulated flow within the sampling footprint of the VPS array for each of the three sites. The selected habitat metrics are then converted into habitat suitability values. The simulated flow through the reach is used to 1) determine the available habitat within the footprint of the VPS array and 2) associate each telemetered fish position with a value of depth and velocity as simulated in the hydraulic model, and the static measured values of substrate type. The sampled areas corresponded to the spatial extent of fish positions calculated by the arrays of telemetry receivers (Fig. 2). The available habitat values were determined by extracting the simulated depth, velocity, and substrate at each grid node within each VPS sampling area over the duration of the flow simulation period at each 12-hour time step. Each telemetered fish position contained a fish ID, a time stamp, and a location in UTM coordinates. A depth, velocity, and substrate type were then assigned to each fish position by interpolating the simulated values at each fish position at the appropriate time step within the simulation. The procedure provides the following: 1) a distribution of depth, velocity, and substrate within the VPS sampling footprint at each simulated time step, and 2) a value of depth, velocity, and substrate for each telemetered fish position.

To develop the habitat suitability values, each depth, velocity, and substrate value assigned to a fish location was weighted by the inverse of the areal fraction of that value in the sampled area as follows. For each modeled time step, the fraction of each habitat parameter by area within the sample footprint was determined. For example, if a sampled area contained only two substrate types, sand and gravel, and sand encompassed 70 percent of the sampled footprint and gravel 30 percent, then the areal fraction of that substrate value for each fish sample found over sand would be 0.7 and over gravel would be 0.3. The fraction by area for depth and velocity were developed by a parallel method, however the distribution of these values in the sampling footprint changed at each modeled time step (i.e., every 12 hours) as the discharge and downstream stage for the model reach changed with time. The suitability curves were then developed by weighting each sampled value by the inverse of the available fraction. Using the example above, we assigned each fish sample over sand a weight of 1/0.7 or 1.42 and each fish sample over gravel would be assigned a weight of 1/0.3 or 3.33. Weighting by the inverse of the availability of each parameter gives more importance to those patches of substrate that are less available yet still selected.

At each sampled site and year, the number of fish sampled and the number of samples per fish varied. To account for this asymmetry in the number of telemetry samples for each fish we additionally weighted each habitat suitability value by the inverse of the fraction that each fish contributed to the total numbers of fish observations by site and year. The effect of weighting by the inverse fraction is to equalize the contribution of each fish to the calculated habitat metrics.

Paired distributions of available and the weighted utilized habitat for each site and each year provide insight into habitat selection. We compared the cumulative distributions of the available and selected habitat data using two-sample Kolmogorov-Smirnov (K-S) goodness-of-fit tests to determine if there were significant differences between the utilized and available habitat. Habitat suitability curves were developed for depth, velocity, and substrate by normalizing the selected values by the largest fraction to produce a suitability value between 0-1 (0 = least suitable, 1 = most suitable).

Weighted useable area

The physical habitat or 'weighted usable area' (WUA, in m^2) at each site was calculated as:

$$WUA = \sum_1^n CSI * a_i \qquad (1)$$

where n is the number of nodes in the computational grid, CSI is the composite suitability index value, and a_i is the contributing area for each grid node (Bovee et al. 1988). The CSI is calculated at each node in the computational grid by converting the simulated habitat metrics to suitability values using the habitat suitability curves and then calculating the geometric mean of these values. The WUA is calculated at each site to assess the quality of the physical habitat as a function of the discharge. The quality as represented by the WUA here is strictly the physical habitat. The WUA in this study was calculated within the entire modeled domain for each reach (approximately 300 meters up and downstream from the VPS). The habitat suitability index values (scaled from 0 -1) associated with the simulated values of depth and velocity (calculated based on a given discharge), as well as observed substrate type, were plotted in each grid node within the reach surrounding each VPS site/year. For each node, the value of the cumulative habitat suitability was calculated as the geometric mean of the three individual suitability values (i.e., mean of velocity, depth, and substrate suitability indices). The WUA was calculated by multiplying the representative area of each 2 x 2 m grid node within each reach by its cumulative habitat suitability index value at a given discharge within 12-hours and summing these values.

RESULTS

Habitat characteristics

The discharge during the flow simulation period was generally similar in 2011 and 2012 with flows varying between 300 – 425 m^3/s. Fig. 3 provides an example of the simulated flow results for depth and vertically-averaged velocity at Site A for the calibrated discharge of 357 m^3/s, as well as the mapped substrate types. The figure captures the unique characteristics of the physical habitat within the VPS footprint relative to the reach as a whole for a single discharge. Site A has a deep pool (~ 11.5 m), downstream from a sharp bend in the river. The deep pool is associated with a bedrock spur protruding into the channel constricting and locally accelerating the flow. Adjacent to the accelerating flow are large lateral recirculation eddies along the channel banks, downstream from the constriction. The VPS footprint generally covers the downstream extent of the pool and the maximum simulated velocities occur upstream from the VPS footprint.

The simulated depth and vertically-averaged velocity values for the grid nodes within the VPS footprint for each study site in each year (termed 'available' habitat), over the duration of the simulated flow, are summarized in Table 1. In general, the distribution of available habitat is different between sites. We show the distribution only for site A (Fig. 4). While most depths at Site A and Site C were between two to nine meters with a steadily decreasing proportion of depths above this level, Site B exhibited a very low relative proportion of depths less than nine meters. A wider distribution of available velocities was noted at Site A and Site C, whereas Site B showed very few available velocities at the extreme ends of the scale. The substrates available within the VPS footprints were primarily gravel followed by sand at Site A, gravel followed by cobble at Site C, and bedrock followed by sand at Site B. Overall, the distribution of available depths was similar between 2011 and 2012 in Site A and Site B. While the shape of the distribution of available velocities was similar between the two years at these sites, the distribution was slightly shifted towards higher velocities in 2011.

Fish positions

A total of 31,871 positions from 39 adult green sturgeon were analyzed in this study (Fig. 2), including 21 males, 2 females, and 16 fish of unknown sex. At the time of tagging, fish had an average fork length of 174.03 ± 13.75 cm (mean ± SD, based on data from 36 fish), ranging from 138 to 201 cm, and girth of 64.15 ± 6.92 cm (mean ± SD, based on data from 36 fish), ranging from 50 to 76 cm. The number of positions per fish ranged from one to 4,572 (mean ± SD: 1593.55 ± 1198.63). The number of total fish positions per site/year ranged from 133 – 23,458 (Table 1); 50.0% of fish were found in at least one VPS site, 42.7% were found in two sites, and 7.5% were found in all three sites.

Green sturgeon were positioned at locations with depths between 0.16 to 11.87 m and velocities between 0.05 and 1.47 m/s (Table 1). The mean depth at fish positions within each VPS site ranged from 4.06 ± 1.63 m (Site C 2012) to 11.28 ± 0.51 m (Site B 2011), with a collective mean of 7.41 ± 2.34 m across all sites and years. The mean velocity at fish positions within each site ranged from 0.90 ± 0.26 m/s (Site C 2012) to 1.21 ± 0.11 m/s (Site B 2011), with a collective mean of 1.01 ± 0.18 m/s across all sites and years. In regards to sturgeon position over substrate type, 30% of all unweighted fish positions occurred over sand, 38% over gravel, 13% over cobble, 1% over boulders, 18% over bedrock, and 0.1% over snags.

Comparison between available and utilized habitat were conducting using utilization data weighted by areal fraction and by fish counts. At Site A, sturgeon utilized deeper habitats than expected based on availability in both years. In 2011, there was a peak in the distribution of available depths at around four meters, while sturgeon showed peak usage at around five meters followed by another peak at around nine meters (Fig. 4A top). There were significantly more shallow depths available within the pool than were occupied by the sturgeon (K-S Test, N=1,242, $p<0.01$). During 2012, the distribution of available depths was similar to 2011, yet again the sturgeon occupied the deeper depths at the sites ranging from four to ten meters with a peak at around nine meters (Fig. 4B top). The difference between depth availability in the pool and that occupied was also significant (K-S Test, N=23,459, p<0.01).

The distribution of velocities present in Site A during 2011 ranged from 0 to 1.6 m/s and was leptokurtotic (skewed to left) with a peak at 1.4 m/s (Fig. 4A middle). The sturgeon were recorded less often in the slower velocities present from 0.0 to 0.4 m/s, but were more often present in the mid velocities from 0.7 to 1.3 m/s during 2011. These differences between the velocities available and those selected were significant (K-S Test, N=1,242, p<0.01). Note that fewer sturgeon were present in water flows >1.4 m/s. At Site A, the difference between the velocities present and those selected by the sturgeon were greater during 2012. Whereas the velocities were relatively uniformly distributed from 0.1 to 1.3 m/s, the sturgeon avoided velocities from 0 to 0.4 m/s and selected velocities exceeding those available from 0.9 to 1.3 m/s (Fig. 4B middle). These differences were also significant (K-S Test, N=23,459, p<0.01).

The sturgeon responded differently relative to substrate at Site A, between the two years of the study. During 2011, the sturgeon were present over sandy bottoms slightly more than the availability of this substrate may predict (Fig. 4A bottom), but during 2012 they were slightly less common over the sandy bottom than expected (Fig. 4B bottom). During 2011, the sturgeon were over gravel less often than the availability of gravel substrate may suggest. However, they were detected more often over a gravel substrate than expected during 2012. Finally, a greater percentage of the sturgeon positions occurred over cobble than expected based on availability during 2011. In conclusion, at Site A the sturgeon selected depths ranging from four to ten meters and velocities of 0.5 to 1.3 m/s. The sturgeon were detected more often over gravel and cobble than was expected based on substrate availability.

At Site B, the relative distributions of utilized depths during 2011 and 2012 exceeded those expected (K-S Test, 2011: N=136, p<0.01, 2012: N=6,857, p<0.01). The sturgeon often occupied waters ten meters or greater in depth. With respect to velocities, the sturgeon also were present more often during the higher velocities in a disproportionate manner to their availability. During 2011, sturgeon were generally present most often in waters 1.1 to 1.3 m/s but with the highest peak in utilization at 0.8-

0.9 m/s. Yet in 2012, they were most present from 0.8 to 1.0 m/s. The frequencies of occupation at the higher velocities were disproportionate to the available velocities (K-S Test, 2011: N=136, p=0.05, 2012: N=6,857, p<0.01). Fish were positioned most frequently over gravel in 2011 and over cobble in 2012, despite low availability of these substrates.

The relative distribution of utilized depths and velocities at Site C in 2012 was similar to the distribution of available habitat, with a peak in sturgeon positioned at depths of three meters and velocities of 0.9 m/s. Utilized habitat values indicated that more fish were positioned at greater depths than expected by availability alone (K-S Test, N=184, p<0.05), but fish did not appear to be selecting particular velocities (K-S Test, N=184, p=0.43), despite a strong usage peak between 1.4 to 1.5 m/s. The sturgeon at Site C were predominantly positioned over cobble and sand at higher levels than expected by availability and over gravel less than expected. Finally, fish also selected sand substrate more often than expected.

Habitat suitability

We determined habitat suitability values by normalizing the weighted depth, velocity, and substrate values associated with fish positions (Fig. 5). Habitat suitability values for depth are shifted towards higher depths at Site B (highest utilization at 10-11 m, Fig. 5B top) and Site A (highest utilization at 8-9 m, Fig. 5A top), but are similar across most depth bins at Site C (highest utilization at 4 and 6 m, Fig. 5C top). Habitat suitability values for velocity are generally right shifted at all sites, with the narrowest range of utilized velocity bins at Site B (highest utilization at 0.9-1.0 m/s, Fig. 5B middle) and the widest range at Site C (highest utilization at 0.8-1.0 m/s, Fig. 5C middle). The velocity bin with the highest utilization at Site A was 1.0 m/s (Fig. 5A middle). The highest habitat suitability values for substrate were cobble at Site C (Fig. 5C bottom), boulder at Site B (with the widest spread in suitability values across substrate types, Fig. 5B bottom), and gravel at Site A (Fig. 5A bottom). When all data were combined, the highest utilization of depth occurred at 8-9 m, for velocity at 1.0 m/s, and for sand and gravel substrate (Fig. 5D bottom). However, it is important to note that the values in the overall plots of suitability values were heavily influenced by the Site A 2012 data set that produced 73.6% of the total positioned fish (Table 1). The selection of depth, velocity, and substrate over time at Site A during 2012 is illustrated in an animation posted on the Biotelemetry Laboratory website (see http://biotelemetry.ucdavis.edu/images/CJFAS_Wyman_etal_Animation_Site_A_2012.mp4

Weighted useable area

Weighted usable areas (WUA) were calculated based on discharge rates, associated cumulative habitat suitability indices, and the area of the reach surrounding each VPS array (Table 2). The discharge range of 288.76 to 670.95 m^3/s during 2011 resulting in a WUA range of 6,003 – 14,303 m^2 at the Site B reach and 5,744 – 10,539 m^2 at the Site A reach. The 2012 discharge range of 217.70 to 433.14 m^3/s produced a WUA range of 5,668 – 7,661 m^2 at the Site C reach, 11,120 – 14,301 m^2 at the Site B reach, and 8,348 – 10,543 m^2 at the Site A reach.

Animations developed to show habitat suitability and WUA over the measured duration of the spawning season for each site and year are available from the authors. A frame from the Site A 2012 animation depicting habitat suitability and WUA during that year's median discharge rate during the sampling period (308 m^3/s) is shown in Fig. 6. Changes in discharge can affect WUA as discharge directly impacts both velocity and depth. For example, as discharge increases, some microhabitat areas may become less suitable (e.g., as velocity or depth values rise above preferred levels) while other areas may become more suitable (e.g., areas that were too shallow or slow to be preferable could increase to desirable levels).

Our results show different relationships between discharge and WUA across the different sites and years, but in general, a negative relationship developed when discharge levels rose above approximately 350 – 400 m^3/s (Fig. 7). This inverse relationship was especially noticeable during the unusually high flow period experienced in early June 2011. The percentage of habitat with medium or high suitability (as a percentage of total WUA with cumulative suitability scores at medium and above levels, >0.5, or only at high levels, >0.7) was similar between Site A and Site C, as was the relationship between discharge and the availability of these habitat suitability levels (Fig. 8). At discharge levels between 240 - 300 m^3/s, the percentage of habitat with at least medium suitability peaked at around 30–35%, while the percentage of highly suitable habitat peaked at around 8 - 10%. Site B had the highest percentage of preferred habitat, with roughly 58% of the reach containing habitat with medium suitability and 27% containing only highly suitable habitat during discharge levels of approximately 350 m^3/s (Fig. 8). In comparison to Site B, Site A and Site C showed little variability in the proportion of habitat with medium or high suitability with changes in discharge. In contrast, Site B displayed sharp increases in overall habitat suitability with increasing discharge up until 350 m^3/s, after which habitat suitability decreases steadily to suitability levels similar to Site A at discharges of 530 m^3/s before falling even lower at higher discharges (Fig. 8).

DISCUSSION

Green sturgeon appear to be selecting particular microhabitats within spawning sites. Habitat suitability values for all three sites combined indicate distinct ranges for the most preferred depth, velocity, and substrate microhabitats. Fish were positioned at depths ranging from 0.16 to 11.87 m, velocities between 0.05 and 1.47 m/s, and a mix of substrate from sand to bedrock. Within these ranges, our findings indicate that the most selected microhabitats included depths between eight to nine meters, velocities between 1.0 to 1.1 m/s, and gravel and boulder substrate. However, when comparing across sites and between available vs. utilized microhabitats within sites, it is evident that green sturgeon displayed more consistent selection for velocities over particular depths or substrates.

Habitat selection

The range of microhabitats over which fish were positioned was similar to the range of microhabitats where green sturgeon eggs were collected in previous studies (USFWS 2013; Poytress et al. 2015), indicating that green sturgeon do spawn over areas containing these microhabitats. The focused use of areas with high depths within our study sites, with highest suitability at eight to nine meters, supports previous research that suggested deep pools were important elements of sturgeon spawning sites. It is possible that there is some density relationship between space available and number of resident spawners. Active tracking telemetry studies showed adult green sturgeon in the upper Sacramento River spent more time in aggregation sites with deep pools greater than or equal to five meters during the spawning season (Thomas et al. 2014). Likewise, green sturgeon egg mat surveys in the same region collected eggs most frequently at locations with depths between 5.5 and 5.8 m (USFWS 2013), with an average depth of 6.4 m (Poytress et al. 2015). Adult movement studies of nDPS green sturgeon have also reported utilization of habitats with deep pools during spawning (Erickson et al. 2002; Benson et al. 2007). Tracking and egg mat studies of Atlantic and white sturgeon indicate that they aggregate to spawn similarly in deep water (Parsley et al. 1994, Hatin et al. 2002, Paragamian et al. 2002, 2009). Gulf sturgeon spawn over a wide range of depths, 2-6 m (Fox et al. 2000). In contrast, lake sturgeon spawn in shallower water, ranging from 0.1-2 m (LaHaye et al. 1992, Auer and Baker 2002, Bruch and Binkowski 2002).

The identified spawning habitat of green sturgeon have been described qualitatively as pools containing high velocity flows (Poytress et al. 2015; USFWS 2013). While adult green sturgeon in our study were positioned over a wide range of velocities, the most preferred velocities were 1.0-1.1 m/s. These values are slightly higher than the velocities observed at green sturgeon egg collection sites (mean 0.8 m/s, Poytress et al. 2015; most frequently observed at 0.7, 0.88, 0.95, and 1.00 m/s, USFWS 2013). Other species of sturgeon also prefer varying flows for spawning. The velocities at Atlantic sturgeon spawning sites in the St. Lawrence River varied similarly from 0.25 m/s at the beginning of the ebb tide to 2.2.m/s at its end (Hatin et al. 2002). The lake sturgeon also spawns over a similar range of velocities from 0.5 to 1.3 m/s (Auer 1996, McKinley et al. 1998). The velocities at white sturgeon egg collection sites are slightly higher between 1.5 m/s and 2.1 m/s in the Columbia River (Parsley et al. 1994).

The National Marine Fisheries Service (NMFS 2009) stated that green sturgeon spawning was thought to occur over a wide range of substrate types from hard sand to bedrock, with cobble as the most preferred spawning substrate (Moyle 2002). While egg surveys conducted by Brown (2007) supported the claim that cobble was most associated with the presence of green sturgeon eggs, Poytress et al. (2015) and USFWS (2013) reported that gravel was the dominant substrate type. Our results support the latter study, as gravel was the most preferred substrates within the sample sites (e.g., selective utilization above levels expected based on availability), followed by sand and boulder substrates. In comparison, white sturgeon eggs were most often found in gravel and cobble in unregulated rivers (Perrin et al. 2003), whereas typical substrates at egg collection sites in rivers regulated by dams ranged from sand (Paragamian et al. 2002) to cobble and boulder (Parsley et al. 1994). Lake sturgeon spawn over substrates of coarse gravel or cobble (Auer 1996, McKinley et al. 1998). Atlantic sturgeon spawn over a substrate of rocks and bedrock in the St. Lawrence River (Hatin et al. 2002).

Selective preferences

Preferences for spawning habitats have been reinforced through an increase in fitness benefits associated with spawning in particular microhabitats. Laboratory studies on the characteristics, movements, and survivorship of sturgeon eggs, embryos, and larvae support the assumption that microhabitat choice by adult fish during spawning strongly influences their reproductive success. Green sturgeon eggs are large, dense, and adhesive (Van Eenennaam et al. 2008; Poytress et al. 2015). Their initial adhesive qualities develop at 5-10 s, but quickly fade until after fertilization when they become highly adhesive (Van Eenennaam et al. 2012). These properties would facilitate the rapid sinking of eggs in the water column post-oviposition and strong adhesion to substrates after fertilization. Additionally, green sturgeon hatchling embryos are very poor swimmers but prefer cover within interstitial spaces between rocks, as do the more active larvae (Kynard et al. 2005). Specific spawning microhabitat preferences may have evolved if survivorship in these early life stages is influenced by the microhabitat where they were initially deposited (Kynard et al. 2005). These assumptions were supported in white sturgeon. McAdam (2011) provided evidence for substrate selection of pre-exogenous white sturgeon larvae, specifically noting preference for gravel and small cobbles with interstitial spaces for hiding. In the presence of suitable substrate, larvae did not move far from the location where eggs are deposited and larval survival was correlated with the ability of larvae to quickly find those substrates after emergence. In both cases, the initial microhabitat preferences by spawning females for egg deposition would strongly impact larvae survival and thus be subject to selection pressures. While these studies focused on fine-scale benefits derived from suitable substrates, interactions with larger scale flow volume and temperatures are also likely to influence larval survival (Mora, 2016).

Our results indicate that adult green sturgeon are selective in their microhabitat use at spawning sites as the types of microhabitat utilized by the fish did not always reflect the relative distribution of available habitat. The technique of weighting utilized fish counts by the availability of microhabitat bins helps elucidate mismatches between available and utilized microhabitat and points towards potential selective preferences for specific microhabitats. During most surveyed periods and sites, fish seemed to select for deeper locations within the VPS footprint than would be expected by chance given the availability of different depths. This apparent pattern was most strongly illustrated at Site A in 2012 (Fig. 4B top), which was also the site and year where most fish were positioned. A similar pattern was seen for velocities as fish appeared to select for higher velocities than expected, except at Site A in 2011 (Fig. 4A top) and Site C in 2012. Evidence for consistent substrate selection was less apparent. For instance, fish seemed to utilize gravel more often than expected at Site B in both years and Site A in 2012, but less than expected at Site A in 2011 and Site C in 2012.

Interestingly, although fish appeared to prefer deeper and faster microhabitats than expected by chance, patterns suggest that selecting for optimum velocities may be more important than optimum depths. Although higher depths than expected were selected within most sites, the most utilized depth bin varied greatly between sites and years, ranging from 3 meters at Site C in 2012 to 11-12 m at Site B in 2011. However, the most preferred velocity bin was similar between all sites and years, ranging from 0.8-0.9 m/s at Site B in 2011 to 1.2-1.3 m/s at Site B and Site A in 2011. Hence, fish may be selecting for depths which produce velocities in a more optimal range, given the discharge conditions at each location. Strong preferences for velocities over depths is not observed in Gulf sturgeon; egg mat surveys reveal that fish spawn over similar velocities and similar depths across years and between sites regardless of river conditions (Flowers et al. 2009).

Changes in river discharge alters the spatial distribution of depth, velocity, and thus substrate composition. As such, the weighted usable area (WUA) of spawning sites, calculated based on the cumulative suitability index scores for these parameters, also fluctuates in relation to discharge. Alterations to discharge patterns through management decisions, drought, and climate change can therefore have large impacts on the amount and quality of preferred spawning habitat (Gillenwater et al. 2006; Tonina et al. 2011). Decisions that reduce preferred spawning microhabitats are likely to decrease sturgeon reproductive success through reduced survivorship of eggs and larvae, ultimately influencing recruitment and population dynamics within species (Flowers et al. 2009). These relationships highlight the importance of predicting the effects of discharge variation on preferred spawning habitat.

Our results showed that the relationship between discharge and WUA was complex and could vary between sites. In some cases, an increase in discharge led to an increase in WUA, while in others it led to a decrease, or no discernible effect. Site A and Site C showed similar responses to discharge in comparison to Site B, most likely due to differences in channel morphology. The two former sites are both characterized by wider channels and gentler bank slopes, while Site B is more channelized with bedrock ledges at the banks. Thomas et al. (2014) documented multiple within-season movements of green sturgeon between spawning and aggregation sites, as did Paragamian et al. (2002) in white sturgeon. It is feasible that these movements could, in part, be driven by the relative increase or decrease in WUA found at each site as a consequence of discharge conditions.

There was a general trend at all sites for discharge and WUA to be inversely related once discharge increased above approximately 350 to 400 m^3/s (Fig. 7). This was most apparent during the high water event in 2011 at Site A and Site B, but was also visible at all sites at the end of the 2012 sampling period. In comparison to Site B, Site A and Site C showed little variation with discharge in the percentage of WUA with at least medium suitability or only high suitability (Fig. 8). Site B experienced a steep rise and fall in the proportion of these quality habitats, with the start of this decrease associated with a rise in discharge above approximately 350 to 400 m^3/s. A similar relationship was reported between discharge and the WUA of highly suitable walleye spawning habitat, although the threshold for the start of decreased WUA with increasing discharge occurred at a lower discharge level (Gillenwater et al. 2006). Overall, Site B had the highest percentage of WUA with medium and high suitability. However, the Site A VPS system recorded many more fish positions than the other two sites. This is likely due to the smaller physical area available within the Site B VPS site due to its more channelized and narrow location; positioning efficiency within this location did not differ noticeably from the other locations.

There are two potential explanations for the inverse relationship between discharge and WUA at higher discharge. One interpretation may be that the higher velocities and depths that occur within the VPS array site during higher discharge levels may be less preferable to green sturgeon for spawning habitat. For instance, the velocities may be too high for the sturgeon to effectively hold their positions over or near the spawning grounds. As a result, the fish may move out of the VPS footprint to locations with more preferable velocities or depths at the margins of the river or upstream or downstream. However, low positioning efficiency associated with high discharge rates may also be influencing the relationship between WUA and discharge. At our locations, there was a trend for positioning efficiency to decrease to very low levels when discharge rose above approximately 350 m^3/s. Our overall positioning efficiencies, as well as the relationship between discharge and efficiency, were similar to other studies (see Steel et al. 2014, which includes an assessment of Site A in 2011). Therefore, it is feasible that green sturgeon were present within the VPS sites yet were not effectively positioned due to the environmental noise associated with the higher flow conditions. Additional studies with an expanded VPS array footprint are required to tease apart these competing interpretations. Furthermore, caution should be taken in transferring any conclusions about the WUA-discharge relationship to other systems as potential differences in habitat suitability criteria may differ between populations or locations (Payne 2003).

A more robust approach is now required which focuses on not only known spawning sites with deep pools, but also on alternative sites which may provide preferred spawning grounds under certain discharge conditions or restoration efforts. The potential suitability of tributaries should also be investigated, given the recent spawning evidence from the Feather River (Seesholz et al. 2015). Indeed, this study highlights the importance of examining microhabitat selection in a variety of conditions. By assessing habitat selection across different sites and years, we were able to better detect patterns in habitat selection, such as the apparent increased importance of velocity microhabitat over depth or substrate. It is important to recognize that habitat site characteristics are derived from complex hydrologic processes that also include variables such as gradient, channel morphology, and the availability of substrates. Given the general assertion that green sturgeon prefer spawning sites with complex hydraulics, future studies should also include a fine-scale examination of vorticity preferences (Wang and Xia 2009). Measuring hydraulic derivatives such as vorticity would provide a more nuanced picture of habitat preferences. Additional monitoring of eggs, larvae, and juveniles may also provide a mechanism for testing if quantity and quality of spawning habitat is in fact a limiting factor to recruitment.

Management Implications

Habitat suitability index models have been utilized to examine riverine habitat suitability or selection in relation to resource management (Brown et al. 2000; Vinagre et al. 2006), flow alternations (Zorn et al. 2012), climate change (Tonina et al. 2011), and dam removal/replacement (Gillenwater et al. 2006; Tomsic et al. 2007). We have used this approach to identify the range of available physical habitat variables within three green sturgeon spawning locations in the Sacramento River. As part of the designation of critical habitat for the sDPS green sturgeon, NMFS (2009) stated that suitable spawning sites should include deep pools (≥ 5 m) with fast, complex flow regimes delivering currents sufficient to impede fungal growth, siltation, and suffocation of eggs. In general, our findings support this characterization and provide important methodologies for precise mapping of selected spawning habitat over a wide range of locations within the putative spawning grounds. It could also be used to more accurately model the effects of management decisions, drought, or climate change on green sturgeon distribution. Indeed, the information from our study could be used in deciding whether to remove weirs on the Feather River to create a secondary spawning area necessary to sustain a robust population of green sturgeon during varying inter-annual climate changes.

This study provides a framework for evaluating behavioral selection for particular environmental parameters on the microhabitat scale during important life stages within species. By examining habitat selection at this fine scale, we gain a more precise understanding of the mechanisms shaping species behavior and ecology over time. In turn, this information can be used to guide efficacious management decisions regarding a variety of important topics from species recruitment to ecosystem restoration. Indeed, this approach can be used to predict the spawning habitat available for spawning over the four-year drought between 2012-2015 at the three sites.

ACKNOWLEDGEMENTS

Any use of trade, firm, or product names is for descriptive purposes only and does not imply endorsement by the U.S. Government. We thank T. Agosta, E. Miller, G. Singer, and A. Steel of the Biotelemetry Laboratory at the University of California, Davis (UCD) and M. Sundman, a fisheries major, California State University, Humboldt. We are also very thankful for the use of fish detections from fish tagged by the California Department of Water Resources, the Oregon Department of Fish and Wildlife, and the Washington Department of Fish and Wildlife. Funding for this study was provided to the Biotelemetry Laboratory at UCD by the United States Bureau of Reclamation (USBOR) in Cooperative Agreement R10AC20012 between UCD and USBOR with A. Peter Klimley, Principal Investigator.

REFERENCES

Adams, P.B., Grimes, C., Hightower, J.E., Lindley, S.T., Moser, M.L., and Parsley, M.J. 2007. Population status of North American green sturgeon *Acipenser medirostris*. Environ. Biol. Fish. 79: 339–356. doi.org/10.1007/s10641-006-9062-z.

Auer N.A. 1996. Response of spawning lake sturgeon to change in hydroelectric facility operation. Trans. Am. Fish. Soc. 125: 66–77. doi.org/10.1577/1548-8659(1996)125%3C0066:roslst%3E2.3.co;2.

Auer N.A, Baker E.A. 2002. Duration and drift of larval lake sturgeon in the Sturgeon River, Michigan. J. Appl. Ichthyol. 18: 557–564. doi.org/10.1046/j.1439-0426.2002.00393.x

Benson, R.L., Turo, S., and McCovey, B.W. 2007. Migration and movement patterns of green sturgeon (*Acipenser medirostris*) in the Klamath and Trinity rivers, California, USA. Environ. Biol. Fish. 79: 269–379. doi.org/10.1007/s10641-006-9023-6.

Bovee, K.D., Lamb, B.L., Bartholow, J.M., Stalnaker, C.B., Taylor, J., and Henriksen, J. 1998. Stream habitat analysis using the instream flow incremental methodology. U.S. Geological Survey, Biological Resources Division, Information and Technology Report USGS/BRD-1998-0004, viii + 131 pp. Available from: https://www.fort.usgs.gov/sites/default/files/products/publications/3910/3910.pdf.

Brown, K. 2007. Evidence of spawning by green sturgeon, *Acipenser medirostris*, in the upper Sacramento River, California. Environ. Biol. Fish. 79: 297-303. doi.org/10.1007/s10641-006-9085-5.

Brown, S.K., Buja, K.R., Jury, S.H., Monaco, M.E., and Banner, A. 2000. Habitat suitability index models for eight fish and invertebrates species in Casco and Sheepscot Bays, Maine. N. Am. J. Fish. Manage. 20**:** 408-435. doi.org/10.1577/1548-8675(2000)020%3C0408:hsimfe%3E2.3.co;2.

Bruch R.M., Binkowski F.P. 2002. Spawning behaviour of lake sturgeon (*Acipenser fulvescens*). J. Appl. Ichthyol. 18: 570–579. doi.org/10.1046/j.1439-0426.2002.00421.x.

Coates, J.H., Hovel, K.A., Butler, J.L., Klimley, A.P., and Morgan, S.G. 2013. Movement and home range of pink abalone *Haliotis corrugata*: implications for restoration and population recovery. Mar. Ecol. Prog. Ser. 486: 189-201. doi.org/10.3354/meps10365.

Conaway, J.S., and Moran, E.H. 2004. Development and calibration of a two-dimensional hydrodynamic model of the Tanana River near Tok, Alaska: U.S. Geological Survey Open-File Report 2004–1225, available from http://pubs.usgs.gov/of/2004/1225/.

CVFED, 2014, Central Valley Floodplain Evaluation and Delineation (CVFED) Program Lidar: Central Valley, data available on the World Wide Web (United States Interagency Inventory), accessed [June 20, 2014]. Available from: https://coast.noaa.gov/inventory/

DeLonay, A.J., Papoulias, D.M., Wildhaber, M.L., Annis, M.L., Bryan, J.L., Griffith, S.A., Holan, S.H., and Tillitt, D.E. 2007. Use of behavioral and physiological indicators to evaluate *Scaphirhynchus* sturgeon spawning success. J. Appl. Ichthyol. 23: 428–435. doi: 10.1111/j.1439-0426.2007.00894.x.

Erickson, D.L., North, J.A., Hightower, J.E., Weber, J., and Lauck, L. 2002. Movement and habitat use of green sturgeon *Acipenser medirostris* in the Rogue River, Oregon, USA. J. Appl. Ichthyol. 18: 565–569. doi.org/10.1046/j.1439-0426.2002.00403.x.

ESRI. 2012. ArcGIS Desktop: Release 10.1. Redlands, CA: Environmental Systems Research Institute.

Flowers, H.J., Pine, W.E., Dutterer, A.C., Johnson, K.G., Ziewitz, J.W., Allen, M.S., and Parauka, F.M. 2009. Spawning site selection and potential implications of modified flow regimes on viability of Gulf sturgeon populations. Trans. Am. Fish. Soc. 138: 1266-1284. doi: 10.1577/T08-144.1.

Fox, D.A., Hightower, J.E., and Parauka, F.M. 2000. Gulf sturgeon spawning migration and habitat in the Choctawhatchee River system, Alabama–Florida. Trans. Am. Fish. Soc. 129: 811-826. doi: 10.1577/1548-8659(2000)129<0811:GSSMAH>2.3.CO;2.

Gillenwater, D., Granata, T., & Zika, U. 2006. GIS-based modeling of spawning habitat suitability for walleye in the Sandusky River, Ohio, and implications for dam removal and river restoration. Ecological Engineering, 28: 311-323. doi.org/10.1016/j.ecoleng.2006.08.003.

Hafs, A.W., Harrison, L.R., Utz, R.M., and Dunne, T. 2014. Quantifying the role of woody debris in providing bioenergetically favorable habitat for juvenile salmon. Ecol. Modell. 285: 30-38. doi.org/10.1016/j.ecolmodel.2014.04.015.

Harrison, L.R., Legleiter, C.J., Wydzga, M.A., and Dunne, T. 2011. Channel dynamics and habitat development in a meandering, gravel bed river. Water Resour. Res. 47: W04513, doi:10.1029/2009WR008926

Hatin, D., Fortin, R., and Caron, F. 2002. Movement and aggregation areas of adult Atlantic sturgeon (*Acipenser oxyrinchus*) in the St. Lawrence River estuary, Quebec, Canada. J. Appl. Ichthyol. 18: 586–594. doi.org/10.1046/j.1439-0426.2002.00395.x.

Heublein J.C., Kelley J.T., Crocker C.E., Klimley A.P., and Lindley S.T. 2009. Migration of green sturgeon, *Acipenser medirostris*, in the Sacramento River. Environ. Biol. Fish. 84: 245–258. doi.org/10.1007/s10641-008-9432-9.

Israel, J.A., Cordes, J.F. Blumberg, M.A., and May, B. 2004. Geographic patterns of genetic differentiation among collections of green sturgeon. N. Am. J. Fish. Manag. 24: 922-931. doi.org/10.1577/m03-085.1.

Kynard, B., Parker, E., and Parker, T. 2005. Behavior of early life intervals of Klamath River green sturgeon, *Acipenser medirostris*, with a note on body color. Environ. Biol. Fish. 72: 85-97. doi:10.1007/s10641-004-6584-0.

LaHaye M., Branchaud A., Gendron M., Verdon R., Fortin R. 1992. Reproduction, early life history, and characteristics of the spawning grounds of the lake sturgeon (*Acipenser fulvescens*) in Des Prairies and L'Assomption rivers, near Montreal, Quebec. Can. J. Zool. 70: 1681–1689. doi.org/10.1139/z92-234.

Legleiter, C.J., Kyriakidis, P.C., McDonald, R.R., and Nelson, J.M. 2011. Effects of uncertain topographic input data on two-dimensional flow modeling in a gravel-bed river. Water Resour. Res. 47: W03518. doi:10.1029/2010WR009618.

Logan, B.L., McDonald, R.R., Nelson, J.M., Kinzel, P.J., and Barton, G.J. 2011. Use of multidimensional modeling to evaluate a channel restoration design for the Kootenai River, Idaho: U.S. Geological Survey Scientific Investigations Report 2010–5213.

Lisle, T.E., Nelson, J.M., Pitlick, J., Madej, M.A., and Barkett, B.L. 2000. Variability of bed mobility in natural, gravel-bed channels and adjustments to sediment load at local and reach scales. Water Resour. Res. 26: 3743-3755. doi.org/10.1029/2000wr900238.

McAdam, S.O. 2011. Effects of substrate condition on habitat use and survival by white sturgeon (*Acipenser transmontanus*) larvae and potential implications for recruitment. Can. J. Fish. Aquat. Sci. 68: 812-822. doi:10.1139/f2011-021.

McKinley R.S., Van Der Kraak G., Power G. 1998. Seasonal migration and reproductive patterns in the lake sturgeon, *Acipenser fulvescens*, in the vicinity of hydroelectric stations in northern Ontario. Environ. Biol. Fish. 51: 245–256. doi:10.1023/A:1007493028238.

Mora, E.A. 2016. A Confluence of Sturgeon Migration: Juvenile Survival and Adult Abundance. Dissertation, University of California, Davis.

Mora, E.A., Lindley, S.T., Erickson, D.L., and Klimley, A.P. 2009. Do impassable dams and flow regulation constrain the distribution of green sturgeon in the Sacramento River, California? J. Appl. Ichthyol. 25 (Suppl. 2): 39–47. doi.org/10.1111/j.1439-0426.2009.01297.x.

Moyle, P.B. 2002. Inland fishes of California, 2nd edition. University of California Press, Berkeley and Los Angeles, CA.

NMFS (National Marine Fisheries Service). 2006. Endangered and threatened wildlife and plants: threatened status for southern distinct population segment of North American green sturgeon. Federal Register 71:67 (7 April 2006): 17757–17766.

NMFS (National Marine Fisheries Service). 2009. Designation of Critical Habitat for the threatened Southern Distinct Population Segment of North American Green Sturgeon. Final Biological Report. Sept 2009.

NMFS (National Marine Fisheries Service). 2015. Southern distinct population segment of the North American green sturgeon (*Acipenser medirostris*). 5-year review: summary and evaluation. Long Beach, California, NMFS, West Coast Region.

Nelson, J.M., and McDonald R.R. 1996. Mechanics and modeling of flow and bed evolution in lateral separation eddies, Glen Canyon Environmental Studies Report, 69 pp. Available from: http://www.gcmrc.gov/library/reports/GCES/Physical/hydrology/Nelson1996.pdf).

Nelson, J. M., McDonald, R. R., Shimizu, Y., Kimura, I., Nabi, M. and Asahi, K. 2016a. Modelling flow, sediment transport and morphodynamics in rivers, in Tools in Fluvial Geomorphology (eds G. M. Kondolf and H. Piégay), John Wiley & Sons, Ltd, Chichester, UK. doi: 10.1002/9781118648551.ch18

Nelson, J. M., Shimizu, Y., Abe, T., Asahi, K., Gamou, M., Inoue, T., Iwasaki, T., Kakinuma, T., Kawamura, S., Kimura, I., Kyuka, T., McDonald, R. R., Nabi, M., Nakatsugawa, M., Simões, F. R., Takebayashi, H., Watanabe, Y. 2016b. The international river interface cooperative: public domain flow and morphodynamics software for education and applications. Adv Water Resour 88.

Paragamian V.L., Wakkinen, V.D., and Kruse, G. 2002. Spawning locations and movement of Kootenai River white sturgeon. J. Appl. Ichthyol. 18: 608–616. doi.org/10.1046/j.1439-0426.2002.00397.x.

Paragamian, V.L., McDonald, R., Nelson, G.J., and Barton, G. 2009. Kootenai River velocities, depth, and white sturgeon spawning site selection – a mystery unraveled? J. Appl. Ichthyol. 25: 640-646. doi.org/10.1111/j.1439-0426.2009.01364.x

Parsley, M.J., Beckman, L.G., and McCabe Jr., G.T. 1993. Spawning and rearing habitat use by white sturgeons in the Columbia River downstream from McNary Dam. Trans. Am. Fish. Soc. 122: 217–227. doi.org/10.1577/1548-8659(1993)122%3C0217:sarhub%3E2.3.co;2.

Parsley, M.J., and Beckman, L.G. 1994. White sturgeon spawning and rearing habitat in the lower Columbia River. N. Am. J. Fish. Manage. 14: 812–827. doi.org/10.1577/1548-8675(1994)014%3C0812:wssarh%3E2.3.co;2.

Payne, T.R. 2003. The Concept of Weighted Usable Area as Relative Suitability Index. IFIM Users Workshop 1-5 June 2003 Fort Collins, CO.

Pikitch, E.K., Doukakis, P., Lauck, L., Chakrabarty, P., and Erickson, D.L. 2005. Status, trends and management of sturgeon and paddlefish fisheries. Fish. Fish. 6: 233-265. doi.org/10.1111/j.1467-2979.2005.00190.x.

Poytress, W.R., Gruber, J.J., Van Eenennaam, J.P., and Gard, M. 2015. Spatial and temporal distribution of spawning events and habitat characteristics of Sacramento River green sturgeon. Trans. Am. Fish. Soc. 144: 1129-1142. doi: 10.1080/00028487.2015.1069213

Scheel, D., and Bisson, L. 2012. Movement patterns of giant Pacific octopuses, *Enteroctopus dofleini*. J. Exp. Mar. Biol. Ecol. 416-417: 21-31. doi.org/10.1016/j.jembe.2012.02.004.

Seesholtz, A.M., Manuel, M.J., Van Eenennaam, J.P. 2015. First documented spawning and associated habitat conditions for green sturgeon in the Feather River, California. Environ. Biol. Fish. 98: 905-912. doi.org/10.1007/s10641-014-0325-9.

Smith, F. 2013. Understanding HPE in the VEMCO positioning system (VPS). V1.0. Available from http://vemco.com/wp-content/uploads/2013/09/understanding-hpe-vps.pdf

Steel, A.E., Coates, J.H., Hearn, A.R., and Klimley, A.P. 2014. Performance of an ultrasonic telemetry positioning system under varied environmental conditions. Anim. Biotelem. 2: 1-15. doi: 10.1186/2050-3385-2-15.

Thomas, M.J., Peterson, M.L., Chapman, E.D., Hearn, A.R., Singer, G.P., Battleson, R.D., and Klimley, A.P. 2014. Behavior, movements, and habitat use of adult green sturgeon, *Acipenser medirostris,* in the upper Sacramento River. Environ. Biol. Fish. 97: 133-146. doi.org/10.1007/s10641-013-0132-8.

Tomsic, C.A., Granata, T.C., Murphy, R.P., and Livchak, C.J. 2007. Using a coupled eco-hydrodynamic to predict habitat for target species following dam removal. Ecol. Eng. 30: 215-230. doi.org/10.1016/j.ecoleng.2006.11.006

Tonina, D., McKean, J., Tang, C., and Goodwin, P. 2011. New Tools for Aquatic Habitat Modeling. *In* Proceedings of the 34th World Congress of the International Association for Hydro- Environment Research and Engineering: 33rd Hydrology and Water Resources Symposium and 10th Conference on Hydraulics in Water Engineering, Brisbane, Australia. Barton, June 26-July 1, 2011. A.C.T.: Engineers Australia. pp. 3137-3144. Available from http://search.informit.com.au/documentSummary;dn=360450124413765;res=IELENG.

USFWS (U.S. Fish and Wildlife Service). 2013. Identification of the instream flow requirements for anadromous fish in the streams within the central valley of California and fisheries investigations. Annual Progress Report, Fiscal Year 2013. U.S. Fish and Wildlife Service, Sacramento Fish and

Wildlife Office, Sacramento, CA 95825. Available from http://www.fws.gov/sacramento/Fisheries/Instream-Flow/fisheries_instream-flow_reports.htm.

U.S. Geological Survey. 2014, National Water Information System data available on the World Wide Web (USGS Water Data for the Nation), accessed [June 20, 2014]. Available from: http://waterdata.usgs.gov/nwis/

Van Eenennaam, J.P. Linares-Casenave, J., Muguet, J.-B., and Doroshov, S.I. 2008. Induced spawning, artificial fertilization, and egg incubation techniques for green sturgeon. N. Am. J. Aquacult. 70: 434-445. doi.org/10.1577/a07-073.1.

Van Eenennaam, J.P. Linares-Casenave, J., and Doroshov, S.I. 2012. Tank spawning of first generation domestic green sturgeon. J. Appl. Ichthyol. 28: 505-511. doi.org/10.1111/j.1439-0426.2012.02012.x.

Vinagre, C., Fonseca, V., Cabral, H., and Costa, M.J. 2006. Habitat suitability index models for the juvenile soles, *Solea solea* and *Solea senegalensis*, in the Tagus estuary: defining variables for species management. Fish. Res. 82: 140-149. doi.org/10.1016/j.fishres.2006.07.011.

Wang, Y. and Xia, Z. 2009. Assessing spawning ground hydraulic suitability for Chinese sturgeon (*Acipenser sinensis*) from horizontal mean vorticity in Yangtze River. Ecol. Model. 220: 1443-1448. doi.org/10.1016/j.ecolmodel.2009.03.003

Wentworth, C.K. 1922. Ecolmodel.2009.03.003. J. Geol. 30: 377-392. doi.org/10.1016/j.

Zorn, T.G., Seelbach, P.W., and Rutherford, E.S. 2012. A regional-scale habitat suitability model to assess the effects of flow reduction on fish assemblages in Michigan streams. J.Am. Water Resour. Assoc. 48: 871-895. doi: 10.1111/j.1752-1688.2012.00656.x.

Table 1. Fish positions, available habitat, and utilized habitat within VPS footprints.

			Site A		Site B		Site C	All Sites
Study year			2011	2012	2011	2012	2012	2011, 2012
Number of fish positions			1,241	23,458	133	6,856	183	31,871
Number of individuals			12	26	3	22	3	39
Available Habitat	**Depth (m)**	Median	4.45	4.16	10.29	9.75	3.86	4.67
		Mean ± SD	4.86 ± 1.95	4.58 ± 1.95	10.03 ± 1.45	9.47 ± 1.42	4.38 ± 2.21	5.56 ± 2.70
		Range	0.72 – 11.64	0.47 - 11.10	3.70 - 12.50	3.26 - 11.46	1.27 - 11.79	0.47 - 12.50
	Velocity (m/s)	Median	1.10	0.86	1.03	0.81	0.93	0.93
		Mean ± SD	0.99 ± 0.45	0.78 ± 0.40	1.04 ± 0.24	0.80 ± 0.17	0.84 ± 0.35	0.87 ± 0.40
		Range	0.001 – 2.02	0.001 – 1.63	0.29 - 1.71	0.21 - 1.15	0.02 - 1.68	0.001 - 2.02
	Substrate (% of total)	Sand	33	33	39.6	39.6	5.3	30.1
		Gravel	63	63	3.5	3.5	55.9	37.8
		Cobble	3	3	9.9	9.9	38.6	12.9
		Boulders	0.5	0.5	1.9	1.9	0.0	1.0
		Bedrock	0	0	45.1	45.1	0.2	18.1
		Snag	0.5	0.5	0.0	0	0.0	.1
Utilized Habitat	**Depth (m)**	Median	4.57	6.71	11.39	10.40	3.58	7.65
		Mean ± SD	4.53 ± 1.13	6.73 ± 1.92	11.28 ± 0.51	10.29 ± 0.75	4.06 ± 1.63	7.41 ± 2.34
		Range	0.16 - 9.38	1.59 - 10.60	7.44 - 11.87	4.34 - 11.37	1.38 - 9.66	0.16 - 11.87
	Velocity (m/s)	Median	1.18	1.05	1.25	0.98	0.99	1.02
		Mean ± SD	1.09 ± 0.27	1.02 ± 0.19	1.21 ± 0.11	0.97 ± 0.08	0.90 ± 0.26	1.01 ± 0.18
		Range	0.06 - 1.47	0.05 - 1.43	0.55 - 1.32	0.24 - 1.12	0.09 - 1.41	0.05 -1.47
	Substrate (% of total)	Sand	24.3	15.4	9.5	8.5	24.3	16.4
		Gravel	48.3	84.3	45.7	20.8	48.3	49.5
		Cobble	27.4	0	19.2	36.3	27.4	22.1
		Boulders	0	.3	25.6	11.5	0	7.5
		Bedrock	0	0	0	22.9	0	4.5
		Snag	0	0	0	0	0	0

Table 2. Weighted usable area (WUA) at VPS locations. WUA was calculated across the full reach of each study location.

	Site A		**Site B**		**Site C**
Study year	2011	2012	2011	2012	2012
WUA (m^2)					
Median	9242	10321	13829	13711	7054
Mean ± SD	9043± 1012	10178± 444	13213± 1980	13249± 1029	7019± 486
Range	5744- 10539	8348- 10543	6003- 14303	11120-14301	5668 - 7661

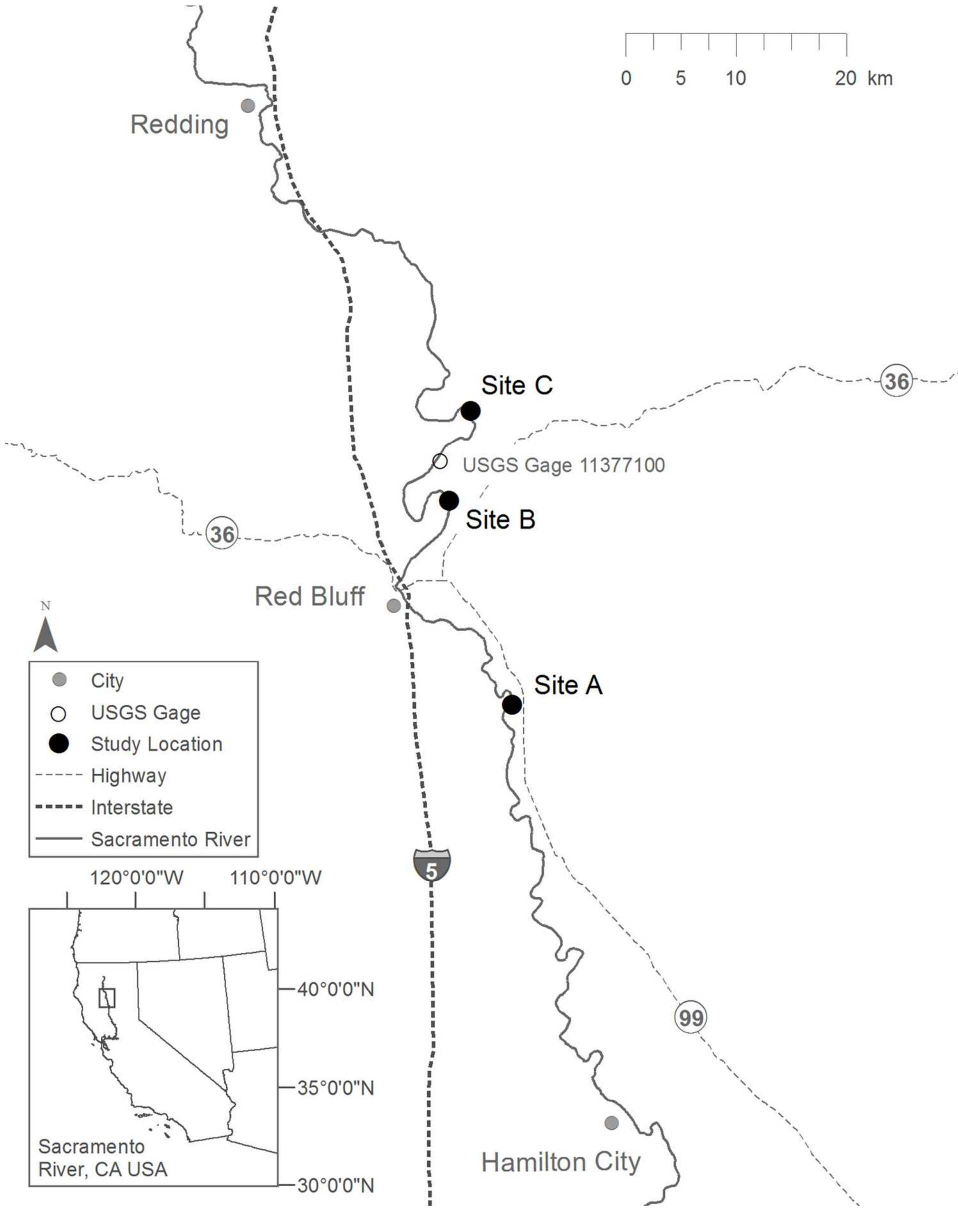

Fig. 1. Map of study reach in the upper Sacramento River, showing the three sites, rkm 377(A), rkm 407.5 (B), and rkm 426 (C). Here, the Sacramento River flows from North to South. The common names of the study sites are not given to protect the spawning habitat for the endangered species from poaching.

127x158mm (300 x 300 DPI)

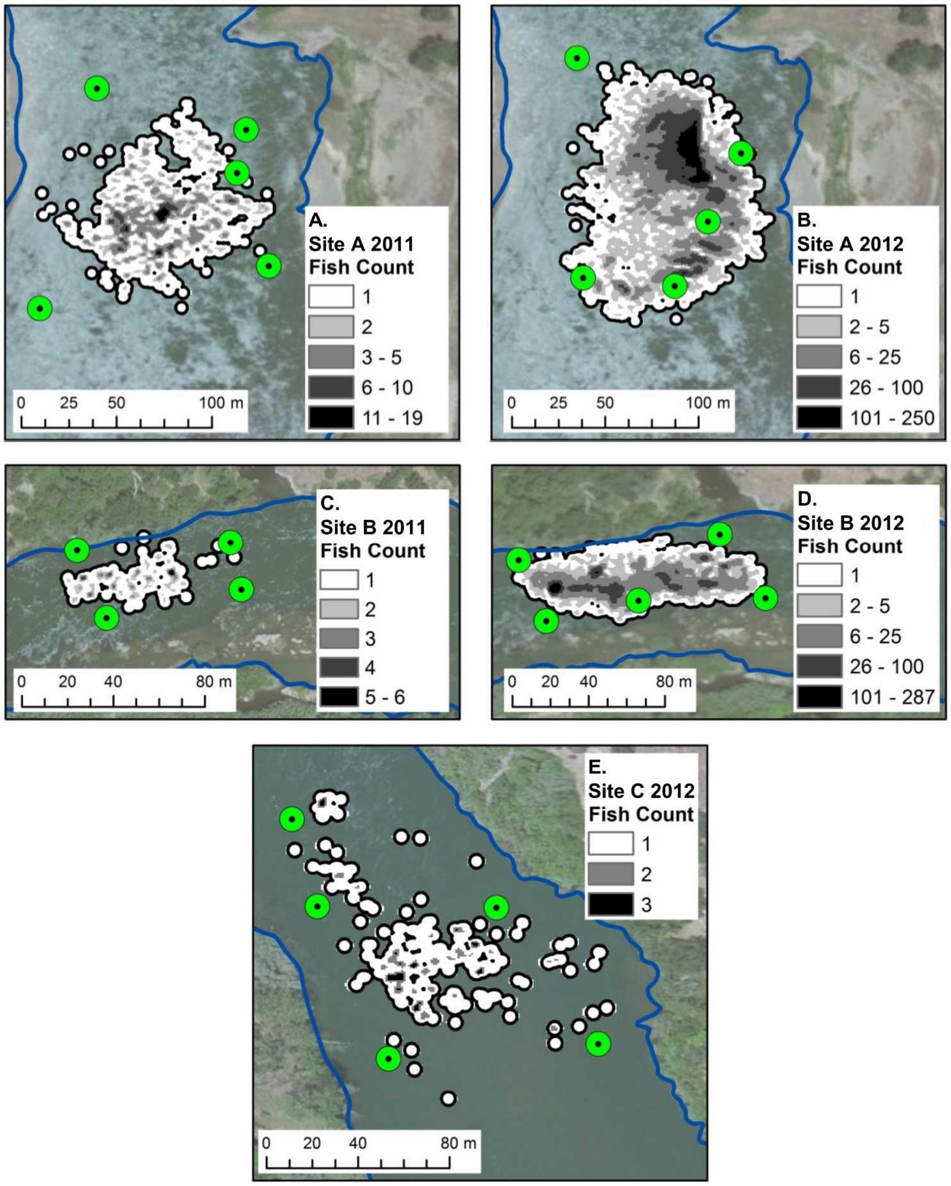

Fig. 2. Fish positions (HPE ≤ 8) within VPS locations at Site A in 2011 (A) and 2012 (B), Site B in 2011 (C) and 2012 (D), and Site C in 2012 (E). Circular green symbols represent VPS receivers and the thick blue line represents the river's edge. Basemaps from ArcGIS Online World Imagery (Sources: Esri, DigitalGlobe, GeoEye, i-cubed, USDA FSA, USGS, AEX, Getmapping, Aerogrid, IGN, IGP, swisstopo, and the GIS User Community).

226x283mm (300 x 300 DPI)

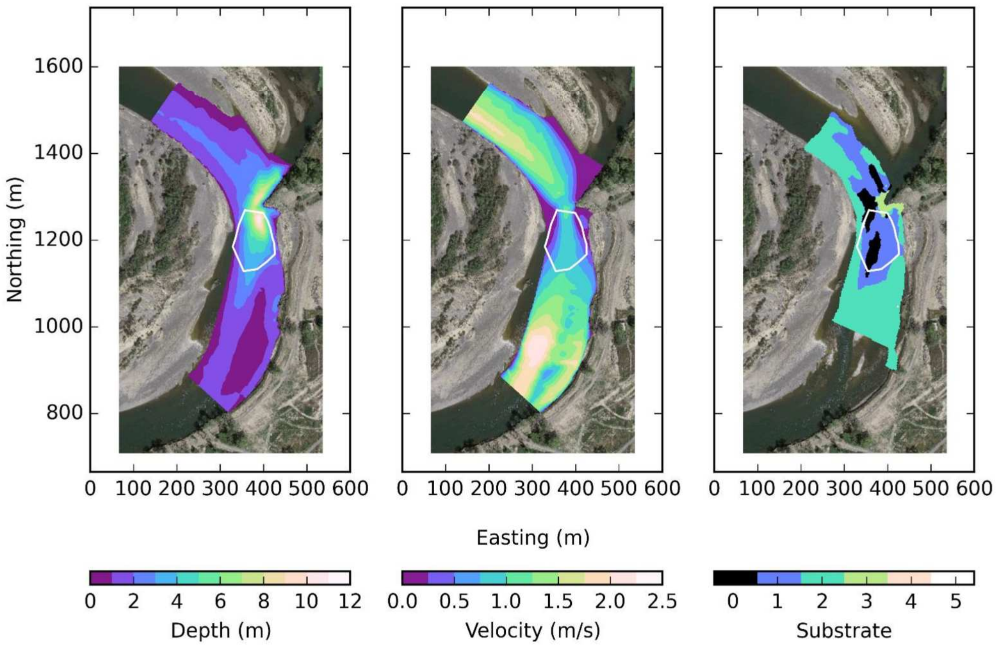

Fig. 3 Depth (left), velocity (middle), and substrate (right) at the Site A reach. Depth and velocity values were calculated during the calibration simulation conducted at a measured discharge of 356.55 m3/s. Substrate values were determined using DIDSON scans (0 = sand, 1 = gravel, 2 = cobble, 3 = boulder, 4 = bedrock, 5 = snag). The polygon outlined in white depicts the outer boundary of fish locations detected by the VPS in 2011 and 2012.

118x76mm (600 x 600 DPI)

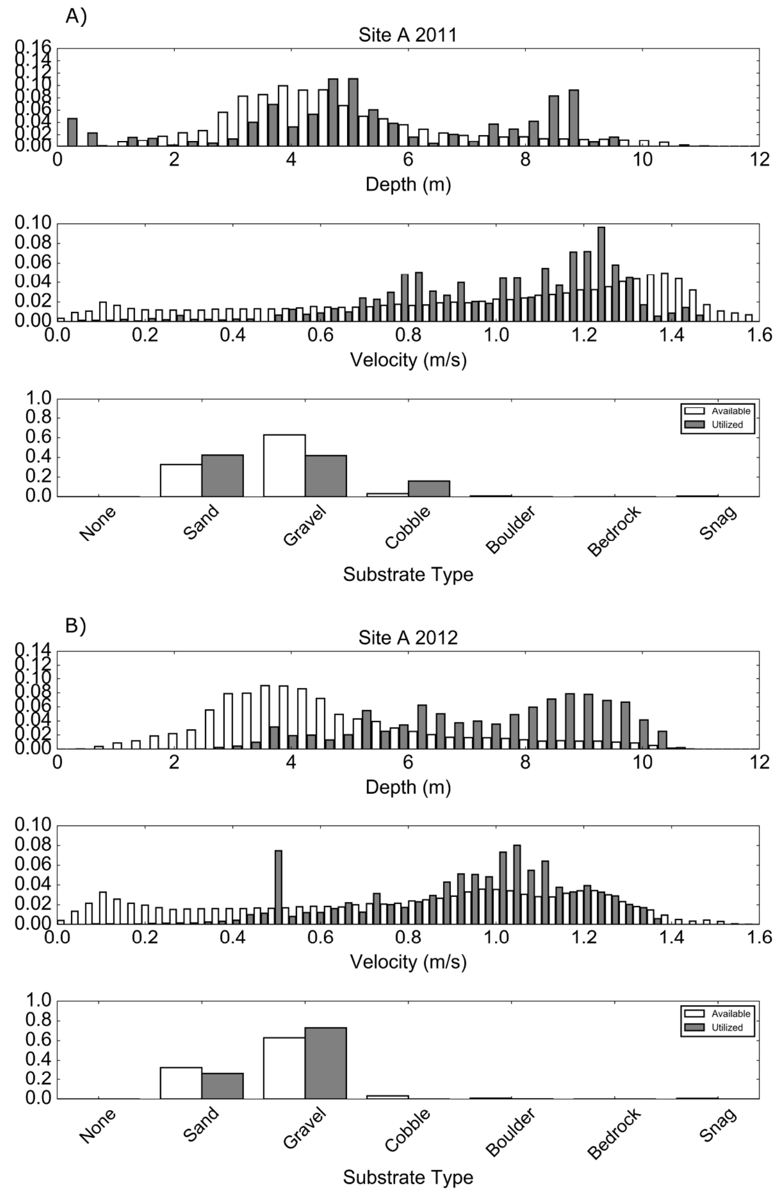

Fig. 4. Available and utilized sturgeon habitat within the VPS sampling area of Site A for 2011 (A) and 2012 (B). The data are weighted (y-axis = fraction of total samples (unitless) according to the number of counts for each fish, thus avoiding one fish having a disproportionate effect on the results of the study.

169x255mm (300 x 300 DPI)

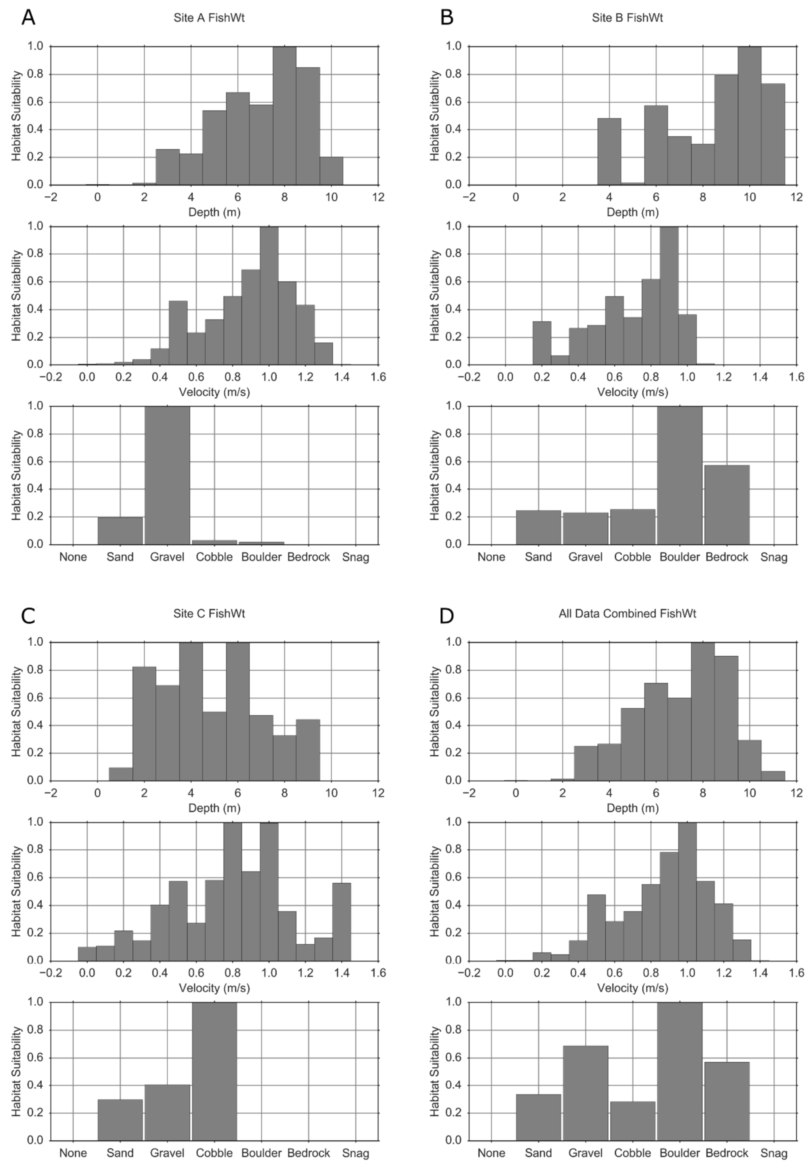

Fig. 5. Histograms of normalized habitat suitability values for depth, velocity, and substrate. Data are presented for Site A with both years combined (A), Site B with both years combined (B), Site C (C), and all sites and years combined (D). The data are weighted according to the number of counts for each fish, thus avoiding one fish having a disproportionate effect on the results of the study.

259x369mm (300 x 300 DPI)

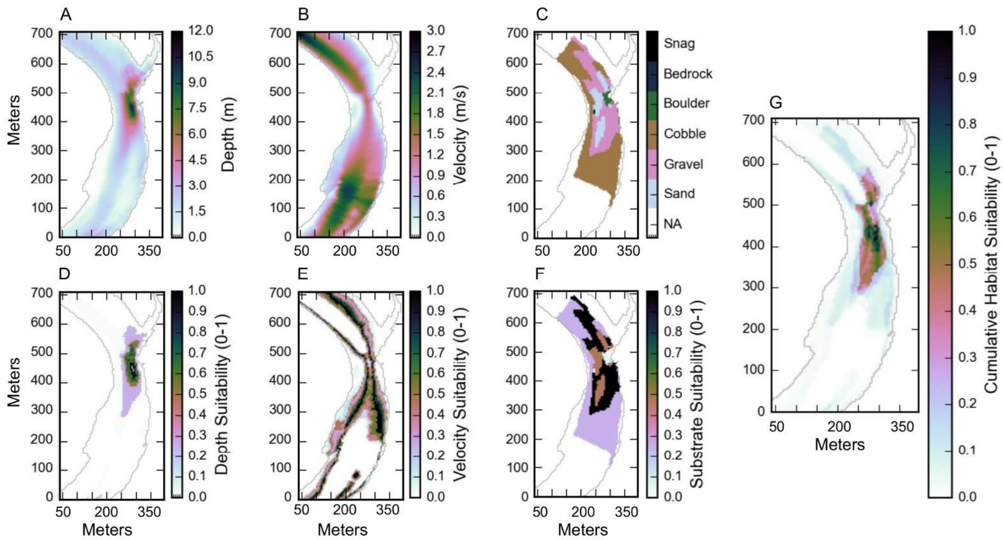

Fig. 6. A frame of the animation of habitat suitability at the Site A reach in 2012. Plots A-C display the simulated depth, simulated velocity, and measured substrate based on a discharge. Plots D-F display the habitat suitability indices for each of the three habitat parameters at this discharge level on a scale of 0 – 1 (1 = highest suitability). Plot G depicts the cumulative habitat suitability index calculated as the geometric mean of the suitability indices of the three habitat parameters.

182x97mm (300 x 300 DPI)

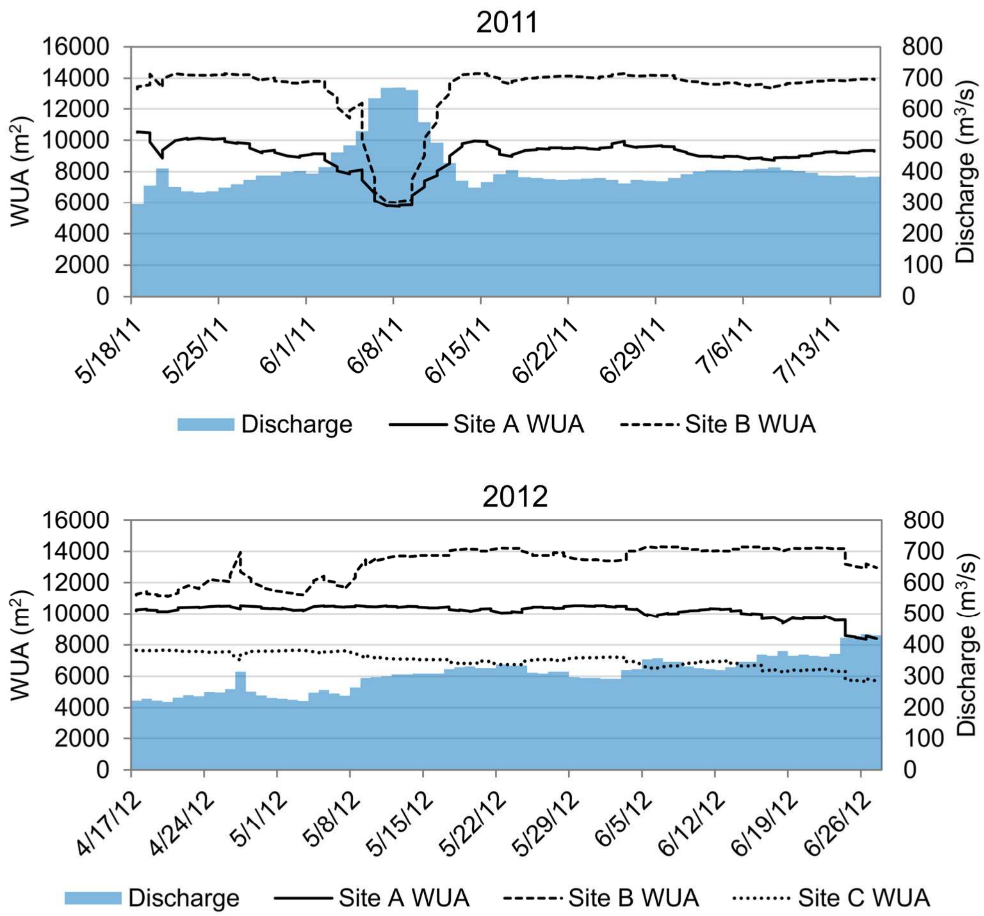

Fig. 7. Weighted usable area (WUA in m2) and discharge (m3/s) over the observed dates in Site A, Site B, and Site C for 2011 (top) and 2012 (bottom)

168x156mm (300 x 300 DPI)

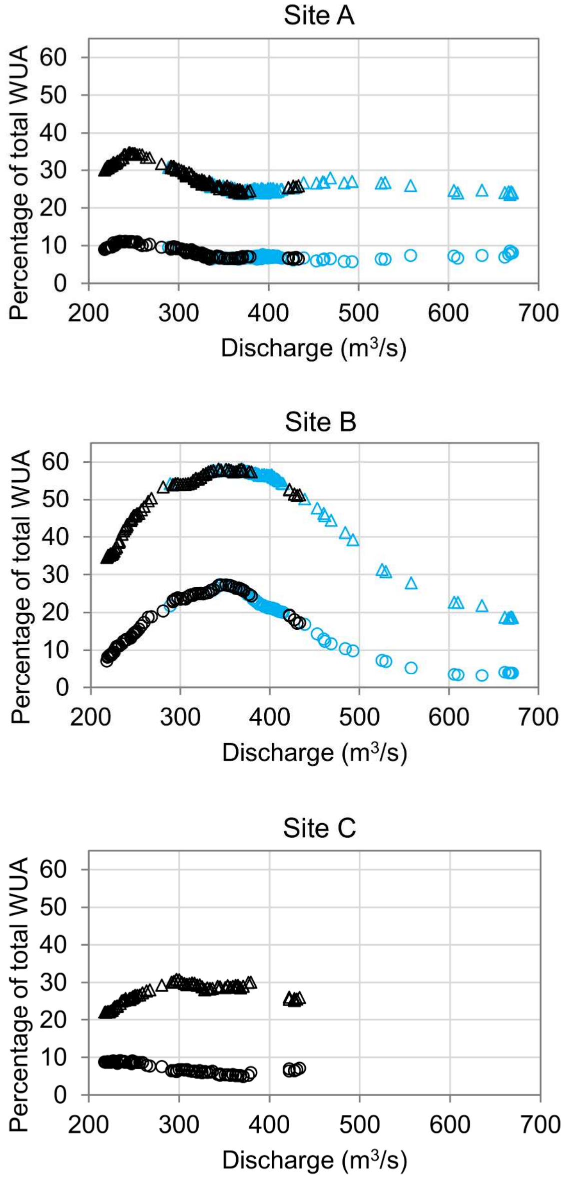

Fig. 8. Relationship between discharge and the percentage of total weighted usable area (WUA in m2) in each study reach with at least medium (triangles) or only highly (circles) suitable habitat for 2011 (blue symbols) and 2012 (black symbols).

177x366mm (300 x 300 DPI)